Understanding the Changes in the Circular Dichroism of Light Harvesting Complex II upon Varying Its Pigment Composition and Organization†

Sofia Georgakopoulou,‡,§ Gert van der Zwan,|| Roberto Bassi,⊥ Rienk van Grondelle,# Herbert van Amerongen,△ and Roberta Croce*,‡,○

Consiglio Nazionale delle Ricerche, Istituto di Biofisica, c/o ITC, Via Sommarive 18 38050 Povo (Trento), Italy, Department of Analytical Chemistry and Applied Spectroscopy and Department of Physics and Astronomy, Faculty of Sciences, Vrije Universiteit Amsterdam, De Boelelaan 1081, 1081 HV Amsterdam, The Netherlands, Dipartimento Scientifico e Tecnologico, Facolta' di Scienze MM.FF.NN, Universita' di Verona, Strada Le Grazie 15, 37134 Verona, Italy, Laboratory of Biophysics, Wageningen University, P.O. Box 8128, 6700 ET, Wageningen, The Netherlands, MicroSpectroscopy Centre, Wageningen University, 6703 HA Wageningen, The Netherlands, and Department of Biophysical Chemistry/GBB, University of Groningen, Nijenborgh 4, 9747 AG Groningen, The Netherlands

Received September 29, 2006; Revised Manuscript Received January 18, 2007

ABSTRACT: In this work we modeled the circular dichroism (CD) spectrum of LHCII, the main light harvesting antenna of photosystem II of higher plants. Excitonic calculations are performed for a monomeric subunit, taken from the crystal structure of trimeric LHCII from spinach [Liu, Z. F., Yan, H. C., Wang, K. B., Kuang, T. Y., Zhang, J. P., Gui, L. L., An, X. M., and Chang, W. R. (2004) *Nature 428*, 287−292]. All of the major features of the CD spectrum above 450 nm are satisfactorily reproduced, and possible orientations of the Chl and carotenoid transition dipole moments are identified. The obtained modeling parameters are used to simulate the CD spectra of two complexes with altered pigment composition: a mutant lacking Chls *a* 611−612 and a complex lacking the carotenoid neoxanthin. By removing the relevant pigment(s) from the structure, we are able to reproduce their spectra, which implies that the alteration does not disturb the overall structure. The CD spectrum of trimeric LHCII shows a reversed relative intensity of the two negative bands around 470 and 490 nm as compared to monomeric LHCII. The simulations reproduce this reversal, indicating that it is mainly due to interactions between chromophores in different monomeric subunits, and the trimerization does not induce observable changes in the monomeric structure. Our simulated spectrum resembles one of two different trimeric CD spectra reported in literature. We argue that the differences in the experimental trimeric CD spectra are caused by changes in the strength of the monomer−monomer interactions due to the differences in detergents used for the purification of the complexes.

Photosynthesis is one of the most important life processes on our planet. The evolution of photosynthetic organisms led to the enrichment of the earth's atmosphere with molecular oxygen, which, in turn, initiated the expansion of life on the surface of the earth. Photosynthetic organisms are equipped with complex systems of membrane-bound pigment proteins that form their light harvesting (LH)[1] antennae and reaction centers (RC), designed to optimize the organisms' performance in capturing and utilizing sunlight. Even though the photosynthetic apparatus of the different organisms is variable, the general process of photosynthesis is rather uniform and involves harvesting of the sunlight and subsequent transfer of the electronic excitation to the RC, where a charge separation is initiated. Through a series of electron and proton transfer steps this eventually leads to the storage of energy in the form of ATP. Under "normal" conditions these primary processes occur with an amazing efficiency.

The plant's major light harvesting complex is the peripheral light harvesting complex LHCII, which is part of the light harvesting antenna of the plant photosystem II (PSII). LHCII is indispensable to the plant's survival, not only for its capacity to gather the sunlight and transfer it to the plant's RC for subsequent conversion into chemical energy but also for its alleged ability of photoprotection in conditions of high

† This work was supported by the European Union, INTRO2 Marie Curie Research Training Network, Human Resources and Mobility Activity Contract MRTN-CT-2003-505069, and by the Provincia Autonoma di Trento, Project SAMBAx2 (to R.C.). R.C. acknowledges support (visitor grant) from the Nederlandse Organisatie voor Wetenschappelijk Onderzoek (NWO).

* To whom correspondence should be addressed. Tel: +31503634214. Fax: +31503634800. E-mail: R.Croce@rug.nl.

‡ Consiglio Nazionale delle Ricerche, Istituto di Biofisica.

§ Current address: M. E. Müller Institute Biozentrum, University of Basel, Klingelbergstrasse 50/70, 4056 Basel, Switzerland.

|| Department of Analytical Chemistry and Applied Spectroscopy, Vrije Universiteit Amsterdam.

⊥ Dipartimento Scientifico e Tecnologico, Universita' di Verona.

Department of Physics and Astronomy, Vrije Universiteit Amsterdam.

△ Laboratory of Biophysics and MicroSpectroscopy Centre, Wageningen University.

○ Department of Biophysical Chemistry/GBB, University of Groningen.

[1] Abbreviations: CD, circular dichroism; LD, linear dichroism; LH, light harvesting; LHCII, light harvesting complex II; PS, photosystem; Chl, chlorophyll; WT, wild type.

10.1021/bi062031y CCC: $37.00
Published on Web 04/03/2007

light (*1*−*6*). LHCII occurs as a heterotrimeric complex of three proteins: lhcb1, lhcb2, and lhcb3, with a stoichiometry of about 7:2:1 in plants (*7*, *8*). Recently, the three-dimensional structure of the complex was determined at atomic resolution (*4*, *6*). LHCII is present in trimeric form in the grana membranes. Each monomer in this trimer comprises 14 chlorophylls (8 Chls *a* and 6 Chls *b*) and 4 xanthophylls. The Chls are arranged in two layers within the membrane, one closer to the stromal surface, with 8 chlorophylls (5 Chls *a* and 3 Chls *b*), and another closer to the lumenal surface, with the remaining 6 Chls. On the stromal side, the average center-to-center distance between two neighboring chlorophylls is 11.3 Å. On the lumenal side, the 6 Chls are arranged in two clusters: one consists of a Chl *a*−Chl *a* dimer, and a second one comprises 3 Chls *b* and 1 Chl *a*. The shortest distance between the two chlorophyll layers is about 13.9 Å (between Chl *b* 609 and Chl *b* 606). The pigment composition of each LHCII monomer is completed with four carotenoids. The two central carotenoids are lutein molecules with an all-*trans* configuration. Their polyene chains form angles of about 59° and 62° with respect to the membrane normal. The third carotenoid, a 9′-*cis*-neoxanthin, is shaped like a bent-over hook, and its polyene chain forms an angle of about 58° with the membrane normal (*9*). Finally, the fourth carotenoid, presumably a violaxantin under low-light conditions, is located at the monomer−monomer interface, and its polyene chain, in an all-*trans* configuration, forms an angle of 34° with the membrane normal. It should be noted that upon isolation of trimers the loss of violaxanthin is common, whereas recombinant complexes reconstituted in vitro in addition lack 1−2 Chls (*8*, *10*, *11*). It was recently shown that the crystal structure corresponds to a dissipative (quenched) state of LHCII (*5*), but modeling studies based on this structure could also explain most spectroscopic features of the isolated, unquenched, trimeric form of LHCII (*12*), suggesting that the unquenched structure is very similar.

As mentioned above, in leaf chloroplasts LHCII appears in a trimeric form, but it is relatively easy to isolate stable monomers (*13*−*15*). These monomers are lacking a few pigments, presumably Chl *b* 601 and the fourth carotenoid violaxanthin (*11*, *15*, *16*). However, their absorption and CD signals, especially in the Q_y region, are very similar, although not identical, to the signals obtained for LHCII trimers (*14*, *17*). The CD signals of LHCII, monomers, trimers, and mutants, are presented frequently in literature and are used to detect structural changes and to study interaction patterns within the complexes (*10*, *15*, *18*, *19*). However, the origin of these CD signals is not fully understood: a change in the CD signal at a certain wavelength does not necessarily represent a change in the arrangement of the pigments absorbing at that particular wavelength, since it can arise from the interaction between transitions that are energetically far apart; i.e., it is possible that a change in the CD signal in the Chl region is a result of a removal or a reorientation of a carotenoid (*20*, *21*). It therefore becomes imperative to theoretically study the origin of the CD spectrum, in order to avoid misinterpretation and to be able to confidently ascribe specific changes in the CD spectrum to disturbances in the structure.

In the past, an excitonic model was used to study the CD spectra of various bacterial LHs, and detailed information on the relation between their structure and their spectroscopic features was provided (*21*−*24*). For example, it was possible to identify the high exciton component of LH2, obtaining an accurate measure for the interaction energy between BChls (*25*); moreover, the red shift of the CD zero crossing with respect to its absorption maximum was explained (*26*); the LH2 carotenoid CD signal was attributed to excitonic interactions (*23*); finally, it became recently possible to elucidate the origin of the fully nonconservative CD signal of *Rhodobacter sphaeroides* LH1 (*21*).

In this work, we try to understand the spectroscopic characteristics of LHCII monomers and mutants with specific structural elements, by performing excitonic calculations of their absorption and CD spectra based on the recently revealed LHCII structure. We thus wish to disentangle the complicated origin of the CD spectrum and make it possible to explain changes in the CD signals.

MATERIALS AND METHODS

Preparation of the Biological Samples. Monomeric LHCII was obtained by overexpressing the wild-type (WT) or mutated (N183V) apoproteins in *Escherichia coli* and reconstituting the pigment−protein complexes *in vitro* with pigments as previously reported (*10*). The "lutein-only" sample was obtained using in the reconstitution a pigment mixture which does not contain neoxanthin (*13*). Native LHCII trimers were obtained from maize plants using the method described in ref *15* but with *n*-dodecyl *β*-D-maltoside (*β*-DM) or *n*-dodecyl α-D-maltoside (α-DM) (*15*).

Experimental. CD spectra were obtained at 8 °C on a Jasco 600 spectropolarimeter. The sample was suspended in 10 mM Hepes, pH 7.6, 0.06% DM, and 20% glycerol. The absorption spectrum was measured on the same sample in an Aminco DW 2000 spectrophotometer. The intrinsic CD signal of the Chls was measured upon temperature denaturation of the LHCII sample at 80 °C.

Theoretical. The CD spectrum is a complex spectroscopic tool that contains a large amount of information. Unfortunately, unraveling this information can be a very difficult task due to the complicated geometric origin of the CD signal: it is the difference in absorption of left (A_L) and right (A_R) circularly polarized light, and it depends on the outer product of the transition dipole moments ($\vec{\mu}_n$ and $\vec{\mu}_m$) of pigments *n* and *m* times the distance between them ($\vec{r}_{nm}$). The equation of the rotational strength $R(\nu)$ that provides the CD signal as a function of the frequency ν is

$$R(\nu) = A_L(\nu) - A_R(\nu) = \frac{-16\pi^2\nu}{9\lambda} \mathrm{Im} \sum_{n,m}^{N} \mathcal{T}_{n,m}(\nu)(\vec{\mu}_n \times \vec{\mu}_m)\cdot\vec{r}_{nm} \quad (1)$$

Here $\mathcal{T}_{n,m}(\nu)$ are the coherence correlation functions:

$$\mathcal{T}_{n,m}(\nu) = \sum_k \langle G(\nu - \nu_{0k}) C_n^k C_m^k \rangle \quad (2)$$

where $\langle\ \rangle$ reflects the averaging procedure over static disorder and ν_{0k} is the frequency corresponding to the transition between excitonic levels 0 and *k*. $G(\nu - \nu_{0k})$ is the line shape function, and C_m^k are the coefficients for the different

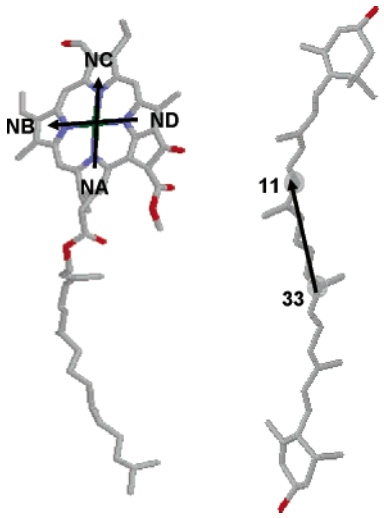

FIGURE 1: Directions of the transition dipole moments of the Chls and carotenoids as assigned in the modeling program.

excitonic states $|k\rangle$ derived by the diagonalization of the system Hamiltonian (see below). The absorption signal, on the other hand, is much simpler to explain since it is described by

$$I(\nu) = A(\nu) = \frac{2\pi\nu}{3} \operatorname{Im} \sum_{n,m} \mathcal{T}_{n,m}(\nu)\vec{\mu}_n \cdot \vec{\mu}_m \qquad (3)$$

where $I(\nu)$ is the oscillator strength; however, it contains less structural information.

For calculating the absorption and CD signals of different monomers of LHCII, we use an excitonic model (*21*−*23*) and start from the recently published 2.75 Å structure of LHCII (*4*). The interactions between all Chl and carotenoid transitions are taken into account, that are crucial for modeling the CD signal of the bacterial light harvesting antenna LH1 (*21*); therefore, the Q_y, Q_x, carotenoid, and Soret regions are included in the calculation. The dipole−dipole interaction operator used is

$$V_{nm} = \frac{1}{4\pi\epsilon_0\epsilon r_{nm}^3}\vec{\mu}_m \cdot \left(1 - 3\frac{\vec{r}_{nm}\vec{r}_{nm}}{r_{nm}^2}\right)\cdot\vec{\mu}_n \qquad (4)$$

where ϵ_0 is the permittivity of the vacuum and ϵ is the relative dielectric constant. The interaction Hamiltonian is given by

$$H = \sum_n^N (E_n|n\rangle\langle n| + \sum_m^N V_{nm}|n\rangle\langle m|) \qquad (5)$$

where E_n is the pigment site energy of each transition. The *y*-transition dipole moments of the Chls (Q_y, B_y) are initially taken along the NB−ND direction of the chlorin ring, in qualitative agreement with experimental (*27*) and theoretical (*12*) linear dichroism (LD) studies on LHCII, while the *x*-transition dipole moments (Q_x, B_x) are along the NA−NC direction (Figure 1). The carotenoids have transition dipole moments oriented along the central conjugated part of the chain as indicated in previous studies (*23*, *28*).

The modeling includes inhomogeneous and homogeneous (σ_{hom}) broadening, the first in the form of a random contribution to the diagonal elements of the Hamiltonian prior to diagonalization and the second by dressing the final stick spectra with Gaussians according to

$$G(\nu - \nu_{0l}) = \frac{1}{\sigma_{\text{hom}}\sqrt{2\pi}} e^{-(\nu-\nu_{0l})^2/\sigma_{\text{hom}}^2} \qquad (6)$$

in order to represent lifetime broadening at high temperatures (*24*, *29*). Since monomers have slightly different composition as compared to trimers, in our modeling program we remove the pigments that do not bind to the monomer [one Chl *b* (601) and one carotenoid (623)]. Although experimental data indicate that this Chl is most likely not present in the monomer, this cannot be stated with certainty. Therefore, modeling was performed also in the presence of Chl 601. The obtained results in the Q_y region were almost identical to those that excluded Chl 601, and some small differences could only be seen in the Soret region (data not shown). In addition, we adjusted the orientations of the transition dipole moments with respect to the molecular framework of the pigments by rotating the transition dipole moments; in order to optimize the simulated spectra, we varied the homogeneous and inhomogeneous broadenings, as well as the site energies of the pigments and the size of their transition dipole moments. In our model, absorption and CD spectra are calculated simultaneously in order to obtain higher accuracy.

RESULTS AND DISCUSSION

The first aim of this work is to explain the CD of monomeric LHCII in different spectral regions and to correlate it with the structure within a monomer, as well as with the most important interactions between the different chromophores. For that purpose the absorption and CD spectra of three different monomeric reconstituted LHCII complexes were investigated: WT LHCII, a mutant (N183V) lacking the red-absorbing Chls *a* 611/612 (nomenclature according to Liu et al. (*4*)), and a complex reconstituted without neoxanthin (named lutein-only) (*13*).

The absorption and CD spectra of monomeric WT LHCII are presented in Figure 2. The Q_y absorption is dominated by two bands at 674 and 653 nm; the first one corresponds to Chl *a* while the second is mainly due to Chl *b*, superimposed on vibronic transitions of Chl *a*. In the blue part of the spectrum, the Chl Soret and carotenoid bands are largely overlapping, and only two clear peaks are visible at 437 and 471 nm with a shoulder around 485 nm. The CD signal is nonconservative and has a "− + −" signature in the Q_y region, while in the blue it features a negative peak at 491 nm with a smaller band at 473 nm and a shoulder at 459 nm and two positive peaks at 444 and 410 nm.

Using the modeling program described in the Materials and Methods section, the absorption and CD signals of a monomer from WT LHCII were calculated (Figure 2). The parameters needed for achieving the modeled spectra are listed in Table 1. Chls *a* and *b* were given different site energies corresponding to their absorption maxima in solution (*30*). Including a further red shift for two or three Chls *a* (Chls 610, 611, and 612), according to several reports in literature (*10*, *12*), did not lead to substantial improvement of the modeled spectra (data not shown). We have also substituted Chl *a* by Chl *b* in sites 613 and 614 to take into account the mixed occupancy of these sites (*10*). Although

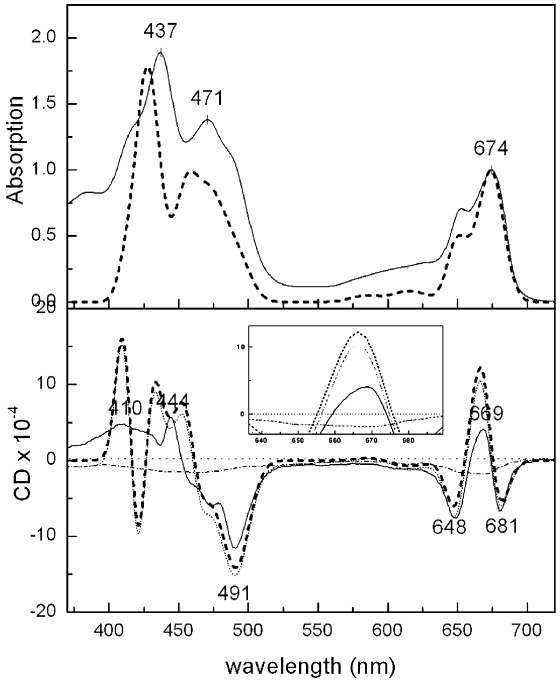

FIGURE 2: WT LHCII monomer measured (solid line) and modeled (dashed line) absorption (top) and CD (bottom) spectra. CD spectra are scaled to the normalized absorption spectra. Also shown are the intrinsic CD signal of Chls (dash-dotted line) and the modeled spectrum with the intrinsic CD added to it (dotted line). The insert shows in more detail the region around 670 nm.

small differences are visible in the individual spectra when the spectra are averaged for the different occupations, the resulting differences are very small compared to the WT; we therefore excluded the mixed occupancy in the model.

Setting the relative dielectric constant to 1, the magnitudes of the Q_y transition dipole moments were taken to be 4 D for Chl *a* and 3.4 D for Chl *b* (*12*, *31*−*33*). The Chl *a*/Chl *b* absorption ratio in the Q_y region is bigger than the measured one because the vibronic Q_y transitions are not included in the modeling. In the modeled CD spectrum all of the major features observed in the measured one are reproduced. One could of course try to optimize the calculated spectra as much as possible by varying bandwidths, site energies, and dipole orientations of individual pigments, but this will introduce too many degrees of freedom to perform a reliable fitting. Instead, we choose to limit the number of parameters and look at more global characteristic features of the spectra. For instance, the properties of all Chls *a* (or Chls *b*) are taken to be identical. Then, it is impossible to get a perfect description of the calculated spectra, especially in the blue region where both the Chls and carotenoids show strongly overlapping absorption bands. One has to compromise between optimizing the modeled intensities and shapes of specific bands. We adjusted the parameters in such a way that a compromise was obtained that simultaneously describes intensities and band shapes in a satisfactory way. We focus mainly on the wavelength region above 450 nm, where the number of overlapping spectra is smaller than below 450 nm. Differences are attributed to the fact that several Chl transitions are not taken into account.

Different dipole orientations have been proposed in the literature for Chl *a* and Chl *b*. Values around −20° with respect to the *y*-axis were reported in refs *34*−*37*, whereas values bewteen 5 and 15° were presented in refs *38*−*40*. Recently, the linear dichroism spectrum of LHCII was modeled (*12*) on the basis of the crystal structure, assuming that the Q_y transition dipole moments are oriented along the *y*-axis. This led to qualitative agreement with the absolute linear dichroism spectrum (*27*), but the absolute value differed, in line with the fact that the Q_y transition dipole moment is not oriented exactly along the *y*-axis. Here we have obtained a good match between measured and calculated spectra using a value of 7.2° for the Q_y transition of Chl *a* (clockwise rotation). This value can be considered to be relatively accurate because rotation of the transition dipole moment strongly influences the calculated CD signals. In Figure 3A,B it is shown how rotations of the transition dipole moment (here Q_y) in the plane of the chlorin ring affect the shape of the CD signal. For example, it can be seen that for rotations of ∼30° there is almost a complete inversion of the CD signal. Already a rotation of 5° leads to strongly reduced similarity with the experimental spectrum. It is also demonstrated (Figure 3C,D) how rotations of the carotenoid transition dipole moments affect not only the carotenoid bands but also the Q_y bands, indicating that carotenoids or other higher transitions can contribute to the nonconservativity in that region (*21*). We should note at this point that the shape of the CD signal does not depend on the absolute orientations of the transition dipole moments but on their mutual orientation.

Finally, a homogeneous broadening of 300 cm^{-1} was used for the Chl Q_y region, while for the Q_x, Soret, and carotenoid regions much larger values were needed, in the order of 700−800 cm^{-1}. The inhomogeneous broadening was set to 300 cm^{-1} for all bands. The high values of (in)homogeneous broadening reflect possible differences in the magnitude and orientation of the transition dipole moments of each pigment involved in the calculations that are very likely induced by the local environment of each pigment.

Summing up, the transition dipole moments and the resulting interaction energies used for the modeling of the LHCII monomer are in agreement with the literature. Minor variations in the magnitude of the transition dipole moments and hence in the interaction energies, as, for example, in ref *12* where smaller values are reported, lead to a change in the size of the signals but do not significantly affect the shape. Here, we have chosen the presented values because they give both qualitatively and quantitatively correct results, in contrast to previous studies that were focusing on the qualitative side alone. In addition, the effect of altering the site energies for certain Chls *a*, to reflect the variable environment of these pigments, was minor. It should be noted that at room temperature the exact values of the site energies are not very important for the shape of the CD spectrum as was theoretically shown in ref *41*. Therefore, a detailed comparison of the used site energies with previously published values is not appropriate. As far as the orientations of the pigments' transition dipole moments are concerned, previous studies are focused mainly on analyzing the LD spectra of the LHCII complexes (*34*−*40*), which are simpler, but contain less structural information. Using CD modeling we are able to significantly narrow down the range of possible transition dipole moment orientations, and yet we are within the limits suggested by the previous studies.

Table 1: Parameters Used for the Modeling of the LHCII Monomers, WT, and Mutants (Figures 2, 5, and 6) and the LHCII Trimer (Figure 7)[a]

	Chls											
	Q_y		Q_x		B_y		B_x		carotenoids			
	a	*b*	*a*	*b*	*a*	*b*	*a*	*b*	0−0	0−1	0−2	0−3
μ (D)	4.0	3.4	1.6	1.4	5.1	6.0	−6.3	−7.1	4.5	×1.05	×0.9	×0.55
E (nm)	670	652	615	583	426.5	455.5	428	464	490	475	445.5	430
σ (cm^{-1})	300		700		800				800			
Δ (cm^{-1})	300		300		500				300			
$\theta(z)$ (deg)	7.2	10	0	0	10	−10	−5.2	−1.0	−20			

[a] *a*, *b*, Chls *a* and *b*; 0−0, 0−1, 0−2, 0−3, vibrational levels of the carotenoids; ×, Franck−Condon (FC) factors for the higher vibrational levels (the transition dipole moment of 0−0 is multiplied by the FC factors to obtain the dipole moments of the higher levels); μ, transition dipole moment; *E*, site energy; σ, homogeneous broadening; Δ, inhomogeneous broadening; $\theta(z)$, rotation around the pigment *z*-axis (for Chls, the *z*-axis is the axis perpendicular to the chlorin ring; for carotenoids, the *z*-axis is the axis perpendicular to the plane defined by the transition dipole moment vector and the long axis of the carotenoid); the minus sign denotes counterclockwise rotation (from the point of view as in Figure 1).

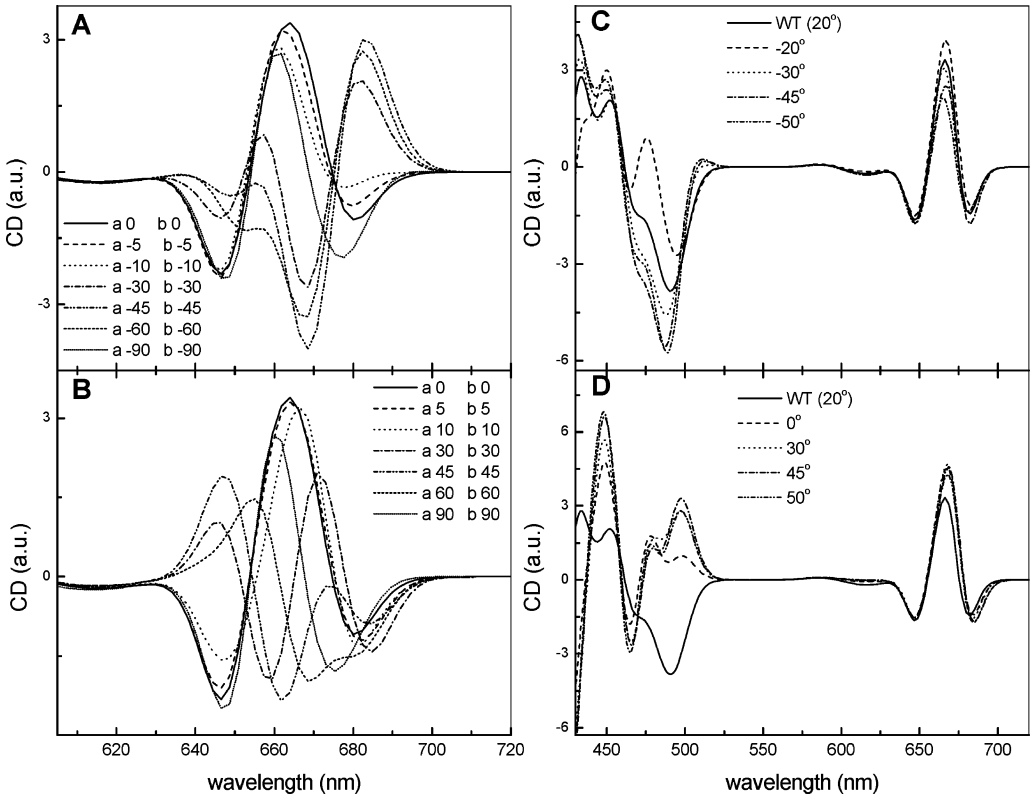

FIGURE 3: (A, B) Effect of the rotations of the Chl Q_y transition dipole moments in the plane of the ring on the Q_y CD signal. (C, D) Effect of the rotations of the carotenoid transition dipole moments in the plane formed by the short (conjugated) and long chain of the molecule on the entire CD spectrum. The minus sign denotes counterclockwise rotation (from the point of view as in Figure 1).

In the modeled spectra the Q_y CD signal is nonconservative but not to the extent observed experimentally. The intrinsic small negative CD signal of Chls in the Q_y region cannot account for this nonconservativity (Figure 2). Mixing with higher states has been held responsible for nonconservativity in the past, in the case of bacterial LH1 (*21*) as well as of BChl dimers (*42*). It was shown above that rotation of the carotenoid transition dipole moments by up to 50° counterclockwise leads to a Q_y CD signal that is as nonconservative as the measured one. However, there is no indication in the literature that the xanthophyll transition dipole moments should be rotated to such an extent; therefore, a different explanation needs to be sought. Possibly the nonconservativity is induced by interactions with protein transitions, which absorb in the blue/UV regions and are still (energetically) relatively close to the Q_y [aromatic amino acids such as tryptophan, tyrosine, and phenylalanine have absorption bands between 250 and 300 nm with significant transition dipole moments (*43*, *44*)]. In addition, peptide bonds could play a role in the nonconservativity of the Q_y since they possess large transition dipole moments, larger than the amino acids, in the far-UV. In any case, pigment−protein interactions are necessary in order to fully explain the LHCII CD spectrum and the complete structure of the pigment−protein complex.

In Table 2 some interaction energies are summarized, and they are in rather good agreement with literature values (*4*, *12*). Small differences are mainly due to the choice of transition dipole moment magnitude and orientation. The strongest interaction between the Chl Q_y transitions occurs between Chls *a* 611/612. Chls *b* 606 and 607 also possess a large interaction in the Q_y region. However, more significant are the interactions between Chl *a* 604 and Chl *b* 606, as well as between Chl *a* 603 and Chl *b* 609. The Q_y transitions of several Chls are quite strongly coupled to the carotenoids. Chl *a* 603 and lutein 621 have the strongest interaction.

Table 2: Major Interaction Energies

transition dipole moment		interaction energy (cm^{-1})
Q_y-Q_y	611*a*−612*a*	131
	604*a*−606*b*	112
	603*a*−609*b*	92
	606*b*−607*b*	66
B_y-B_y	604*a*−606*b*	253
	611*a*−612*a*	211
	603*a*−609*b*	178
	606*b*−607*b*	169
	610*a*-608*b*	120
B_x-B_x	606*b*−607*b*	452
	604*a*−606*b*	−380
	611*a*−612*a*	214
	613*a*−614*a*	−129
Q_y-Q_x	614*a*−613*a*	43
	606*b*−607*b*	34
Q_y-B_y	604*a*−606*b*	194
	611*a*−612*a*	166
	607*b*−606*b*	126
Q_y-B_x	606*b*−607*b*	−183
	614*a*−613*a*	−163
B_y-B_x	612*a*−613*a*	−200
	606*b*−607*b*	−195
	606*b*−604*a*	−190
	607*b*−606*b*	175
car0−0 − Q_y	620*lut*-610*a*	−44
	621*lut*-603*a*	239
	622*nex*-608*b*	90
car0−0 − Q_x	620*lut*-612*a*	−176
	621*lut*-603*a*	−76
car0−0 − B_y	620*lut*-610*a*	61
	621*lut*-603*a*	290
	622*nex*-608*b*	229
car0−0 − B_x	620*lut*-612*a*	679
	621*lut*-603*a*	260
	622*nex*-608*b*	221

Neoxanthin also shows significant interaction with Chl *b* 608. Finally, the transitions in the Soret region interact strongly with transitions in the Q_y, and the most significant pair in this case is the Q_y transition of Chl *a* 604 with the B_y of Chl *b* 606 followed by the interaction Q_y transition of Chl *b* 606 with the B_x of Chl *b* 607.

As mentioned in the introduction the CD signal in a specific spectral region is the result of excitonic interactions between all of the pigments in the monomer. For example, it was shown that changes in the rotations of the pigments' transition dipole moments affect the CD signal in the entire spectral range; especially higher transitions can affect the lowest ones significantly. In order to make the role of the excitonic interactions in the formation of the final CD signals more clear, we show 3D plots of the mutual rotational strength between the chromophores in specific wavelength regions (Figure 4). From these plots we can identify the interactions that play a role in the formation of the CD signal. At 680 nm, for example, the negative CD is mainly the result of a negative contribution from the Q_y transitions of Chls 611 and 612; however, there is also a relatively strong positive contribution from the Q_y of Chls 604 and 606. Moreover, the effect caused by the interaction between the Chls Q_y and Soret regions, as well as the Q_y and the carotenoids, is rather prominent. The other plots reveal similar effects. For details on the major contributions see Table 3. The spectra of the N183V mutant are shown in Figure 5. Compared to the WT protein this mutant presents significant spectral differences in the Q_y region: the main absorption band is shifted 2 nm to the blue while the red-most negative CD band has disappeared almost completely, and the positive one has shifted to the red by 3 nm. The loss of the negative CD band indicates that the rotational strength in that region stems mainly from the interactions induced by the 611/612 pair. In the Soret and carotenoid regions there are also significant differences, namely, an intensity increase of the 485 nm shoulder of the absorption band, accompanied by a decrease of the 473 nm CD band and an increase of the 459 nm shoulder that is now very clear and appears as a separate, small band.

In order to explain these differences, we tried to model the spectra: A new input pdb file was created, from which the 611/612 Chls were removed, and the positions of all of the other pigments were preserved. All of the parameters in the modeling program were kept unchanged. In Figure 5 the absorption and CD spectra of the N183V mutant are compared to those of the WT. The main changes between the N183V mutant and the WT spectra mentioned above are reproduced in our calculations, confirming that they are the result of the interactions between the pigments and not of a structural rearrangement in the complex. Although we are probing pigment−pigment interactions, it is clear that a change in the structure of the complex would almost unavoidably lead to changes in the relative distances and orientations of the pigments and thus in the CD spectrum. The pigments and their interactions can thus be used to monitor structural changes (*45*, *46*). Therefore, it is clear from the CD calculations that a large part of the red-most absorption in LHCII is due to the 611/612 pair, in agreement with earlier results (*10*).

We proceeded by modeling another stable altered complex (the lutein-only complex) in which the neoxanthin molecule is absent (Figure 6). This complex shows no significant changes in the positions of its absorption and CD bands compared to the WT monomer, whereas the Q_y absorption bands are slightly broadened. The CD signal in this region shows small changes, mainly a decrease of the 665 and 647 nm bands, accompanied by small shifts, showing that the pigments that are mainly affected by the removal of neoxanthin are Chls *b* (*9*). In the Soret and carotenoid region the 485 nm shoulder that has increased intensity in the case of the N183V mutant is now small and difficult to distinguish. The CD signal shows significant changes, with the main negative band decreasing and the 473 nm shoulder gaining intensity. The spectra were modeled by creating a pdb file that lacked the carotenoid neoxanthin (622), while keeping all of other parameters in the modeling unchanged. In this way, the essential differences between the mutant and the WT signals in the Soret/carotenoid region of the spectrum were reproduced. In the Q_y region no significant differences exist between the modeled WT and lutein-only complex spectra. This implies that the slight differences in the experimental spectra observed in this region (all of the main features are the same) are due to some small differences in the pigments' structure, in agreement with previous conclusions (*13*).

In conclusion, the CD calculations reproduce the main spectral changes that are experimentally observed upon changing both the Chl and carotenoid content of LHCII, and therefore it can function as a sensitive tool to pinpoint specific excitonic interactions and thus also to obtain

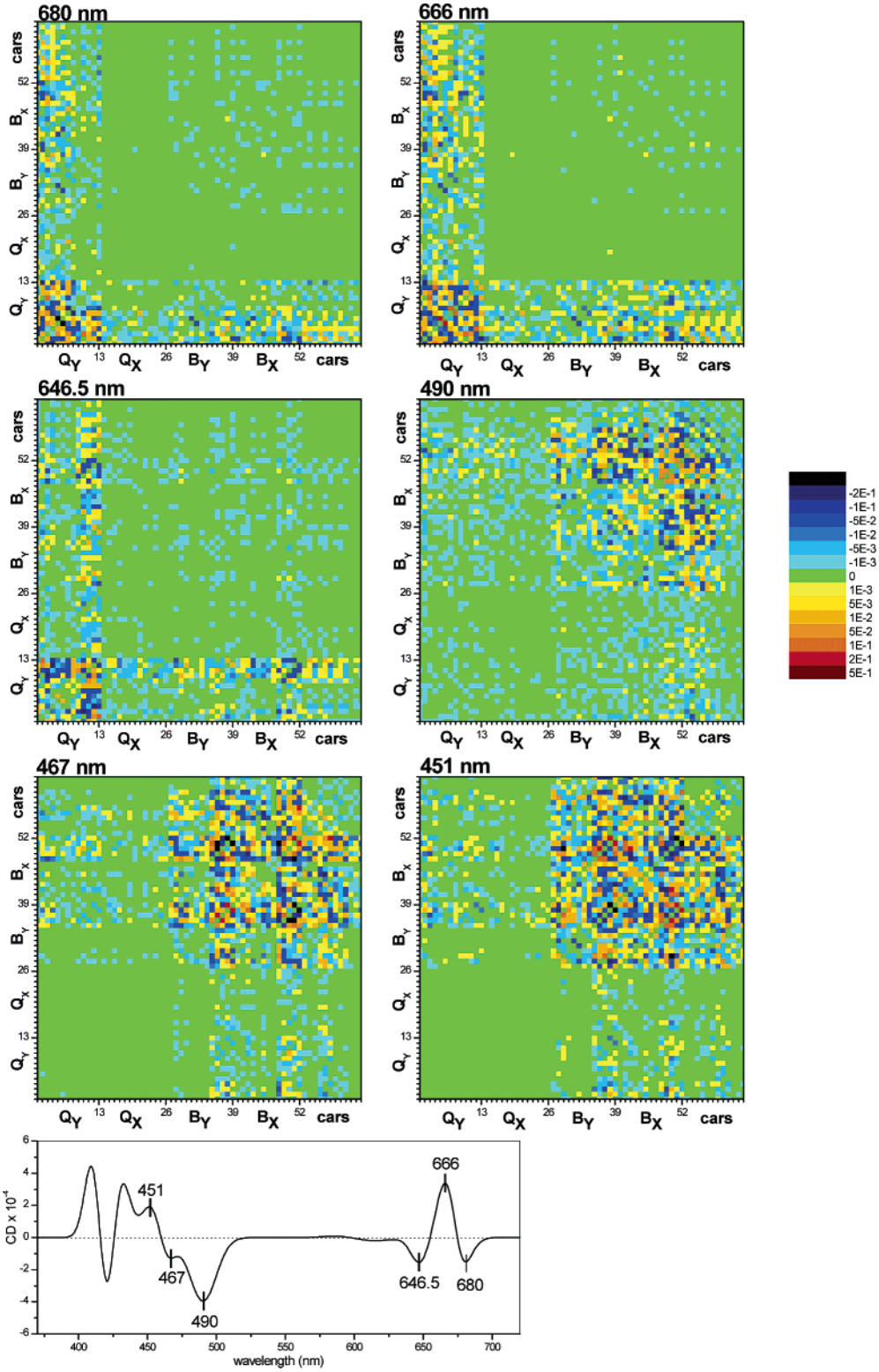

FIGURE 4: 3D plots of the rotational strength matrix (i.e., the rotational strength for every pair of pigments in the modeled complex) at different parts of the WT LHCII monomer spectrum. The *x*- and *y*-axes reflect each pigment's transition dipole moments. In particular, numbers 1−13 are the Q_y transition dipole moments of Chls 602, 603, 604, 610, 611, 612, 613, 614 (*a*'s), 605, 606, 607, 608, 609 (*b*'s). Similarly, 14−26 reflect the Q_x, 27−39 the B_y, and 40−52 the B_x. Numbers 53−55 reflect the 0−0 carotenoid transition of lutein 1, lutein 2, and neoxanthin, respectively, 56−58 the 0−1, 59−61 the 0−2, and 62−64 the 0−3.

structural information. This allows us to inspect the origin of the changes in the CD spectrum upon trimerization and to try to understand the differences between the various CD spectra that have been published in the literature (*17*, *47*−*50*). In Figure 7A the experimental monomer CD spectrum is given together with two different trimer spectra. The two trimers were purified with different procedures and in the presence of different detergents. It should be noted that the LHCII *β*-DM spectrum has been reported many times for trimers with and without violaxanthin. The LHCII α-DM spectrum has only been reported once in the literature for trimers that contain all carotenoids. The main difference

Table 3: Contributions to Rotational Strength[a]

	main contributions	other contributions
680 nm	611*a* Q_y−612*a* Q_y (−0.3)	613*a* Q_y−614*a* B_x (0.027)
	613*a* Q_y−614*a* Q_y (−0.17)	604*a* Q_y−605*b* B_x (0.022)
	604*a* Q_y−606*b* Q_y (0.13)	603*a* Q_y−609*b* B_y (−0.017)
	603*a* Q_y−609*b* Q_y (−0.12)	603*a* Q_y−Lut2 (0.016)
666 nm	611*a* Q_y−612*a* Q_y (0.27)	613*a* Q_y−614*a* Q_x (0.017)
	613*a* Q_y−614*a* Q_y (0.16)	610*a* Q_y−602*a* B_x (0.018)
	603*a* Q_y−609*b* Q_y (−0.11)	610*a* Q_y−608*b* B_y (0.027)
	604*a* Q_y−606*b* Q_y (0.1)	603*a* Q_y−Lut2 (0.018)
646.5 nm	604*a* Q_y−606*b* Q_y (−0.15)	604*a* Q_y−607*b* B_x (−0.03)
	603*a* Q_y−609*b* Q_y (0.14)	606*b* Q_y−607*b* B_x (−0.038)
	610*a* Q_y−608*b* Q_y (−0.12)	605*b* Q_y−606*b* B_x (−0.026)
		609*b* Q_y−Lut2 (0.017)
490 nm	612*a* B_x−Lut1 (−0.13)	603*a* Q_y−Lut2 (−0.012)
	605*b* B_x−607*b* B_x (0.08)	606*b* B_x−603*a* Q_y (0.01)
	606*b* B_x−607*b* B_x (0.08)	604*a* Q_y−612*a* B_x (0.01)
	608*b* B_x−Nex (−0.07)	
467 nm	608*b* B_x−609*b* B_y (−0.36)	604*a* Q_y−605*b* B_x (−0.015)
	608*b* B_y−609*b* B_y (0.35)	606*b* Q_y−607*b* B_x (0.01)
	608*b* B_x−609*b* B_x (0.26)	609*b* Q_y−608*b* B_x (0.01)
	606*b* B_y−607*b* B_x (−0.26)	
	606*b* B_y−608*b* B_x (−0.26)	
451 nm	608*b* B_x−609*b* B_y (0.37)	604*a* Q_y−607*b* B_x (0.026)
	607*b* B_x−604*a* B_x (0.34)	604*a* Q_y−607*b* B_y (−0.012)
	608*b* B_x−609*b* B_x (−0.3)	603*a* Q_y−608*b* B_y (0.012)
	607*b* B_x−606*b* B_y (0.29)	

[a] Contributions to the rotational strength at different wavelengths of various pairs of transition dipole moments (see also Figure 4). In parentheses the relative contributions are given.

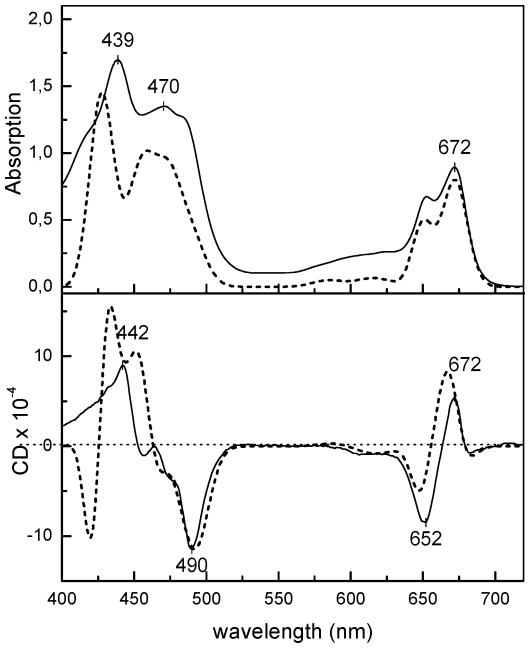

FIGURE 5: N183V mutant (a LHCII monomer lacking Chls *a* 611−612) measured (solid line) and modeled (dashed line) absorption (top) and CD (bottom) spectra. Measured and modeled spectra are scaled on the WT LHCII monomer measured and modeled normalized absorption, respectively.

between the various spectra resides in the relative amplitudes of the two negative CD bands around 470 and 490 nm. Upon trimerization the intensity of the first one increases and the other one decreases. In order to try to understand these differences, we created a monomer structure that contains all of the pigments found in the trimeric structure (trimer-like monomer) (*4*); i.e., we included Chl *b* 601 and violaxanthin. As can be seen in Figure 7B, this leads to some changes in the blue region of the CD spectrum. The negative

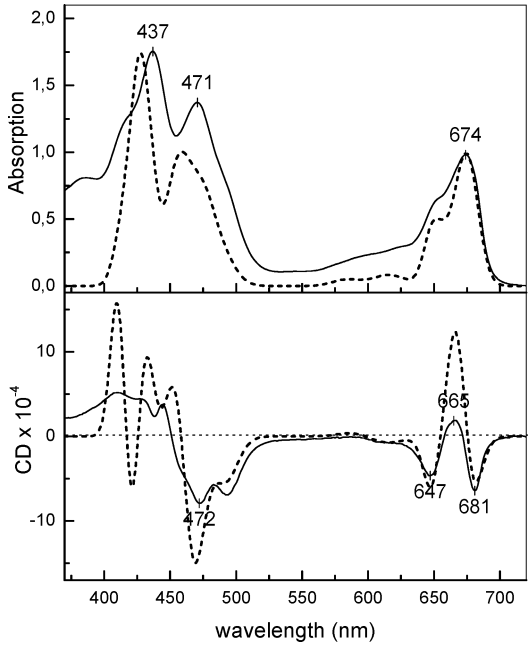

FIGURE 6: Lutein-only complex measured (solid line) and modeled (dashed line). Measured and modeled spectra are scaled on the WT measured and modeled normalized absorption, respectively.

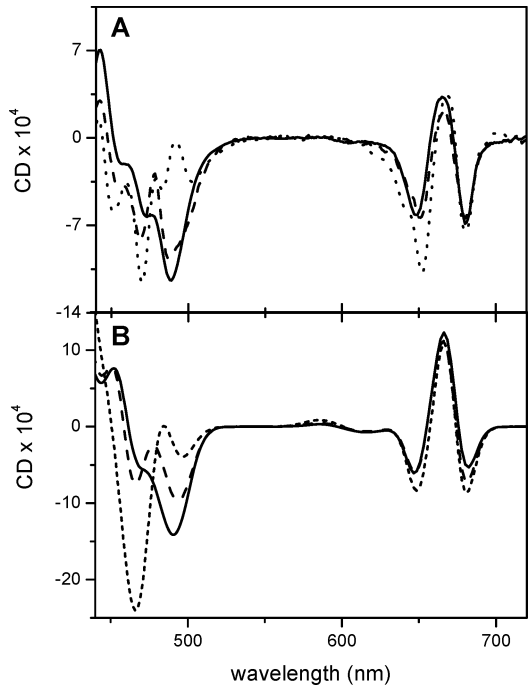

FIGURE 7: (A) Measured CD spectra of a monomer (solid line), a trimer prepared in β-DM (dashed line), and a trimer prepared in α-DM (dotted line). (B) Modeled CD spectra of a monomer (solid line), a trimer-like monomer (dashed line), and a trimer (dotted line).

band at 491 nm loses rotational strength in favor of the shoulder at 467 nm, which becomes a clear band, and these two bands move away from each other. Consequently, the differences between monomeric and trimeric spectra seem to be at least partly due to intramonomer interactions.

Next, the CD signal of the whole trimer was calculated (Figure 7B). The 491 nm band is even smaller and is located further to the red while the 467 nm band has increased and is now the main negative band in that region. Thus, it is clear that the interactions between monomers contribute

significantly to the change in the CD spectrum in this region. The simulated spectrum resembles much better the α-DM spectrum than the *β*-DM spectrum. At present we can only speculate about the origin of the differences between the two types of experimental trimer spectra. The most likely explanation is that the monomer−monomer interactions are different in these preparations, since these interactions have the strongest effect on the ratio of the two negative CD bands. Although the presence/absence of violaxanthin influences the ratio of the two bands, there is only a minor effect in the case of trimers. It is much more likely that the difference in the spectra is due to differences in the intermonomer interactions. This would imply that the trimer isolated with α-maltoside (*15*) shows an organization that is in better agreement with the crystal structure than the trimers isolated with other detergents. It should be realized that most other spectroscopic measurements have been performed with trimers isolated with detergents other than α-maltoside. If indeed the monomer−monomer interactions are different in these preparations, this is also likely to lead to different equilibration times of excitations over the trimer. These equilibration times can be measured with singlet−singlet annihilation experiments (*51*), and it seems interesting to use this technique to test the above hypothesis.

CONCLUSIONS

The modeling of the absorption and CD signals of LHCII monomers and trimers, based on the known crystal structure (*4*), has provided valuable insight into the specifics of the structure of these complexes. Using the dipole−dipole approximation, we were able to reproduce the main features of the CD spectra of different LHCII complexes (monomer, trimer, and mutants). The first conclusion we could draw is that the orientations of the Q_y transition dipole moments of Chls *a* and *b* are nearly parallel to their *y*-axis (NB−ND direction), while the orientation of the S_0-S_2 transition of the xanthophylls is nearly parallel to their central conjugated part. On the other hand, we could not obtain conclusive results regarding the nonconservativity displayed in both the Soret/carotenoid and Q_y regions of the LHCII CD signal; taking into account only the transitions above 400 nm does not render the CD signal significantly nonconservative, which indicates that the nonconservativity is due to protein−pigment interactions and/or higher pigment transitions.

As far as the other two monomeric complexes are concerned (N183V mutant and lutein-only complex), modeling of their CD signals provided structural information. The altered CD of the mutant N183V could be successfully reproduced, indicating that the mutation only has a local effect and does not change the overall conformation: the excitonic interaction between Chls 611 and 612 appears to be responsible for the red-most absorption and CD band. Moreover, the difference in CD due to the absence of neoxanthin could be effectively mimicked by omitting neoxanthin from the structure, indicating that the removal of this pigment does not cause major overall changes.

The final conclusion concerns the trimer vs monomer CD signals. The experimentally observed reversal of the intensity of the negative CD bands around 470 and 490 nm upon monomerization/trimerization is also observed in our simulations, indicating that it is due to interactions between pigments in different monomeric subunits. The calculated trimer spectrum resembles the experimental spectrum reported in ref *15* on LHCII trimers purified by mild detergent treatment. The other experimental spectra presented in the literature show relative intensities that are intermediate between those of the simulated monomer and trimer, suggesting that the monomer−monomer interaction can be weakened by detergents.

REFERENCES

1. Cogdell, R. J. (2006) The structural basis of non-photochemical quenching is revealed?, *Trends Plant Sci. 11*, 59−60.
2. Fleming, G. R., and van Grondelle, R. (1994) The primary steps of photosynthesis, *Phys. Today 47*, 48−55.
3. Horton, P., Ruban, A. V., Rees, D., Pascal, A. A., Noctor, G., and Young, A. J. (1991) Control of the light-harvesting function of chloroplast membranes by aggregation of the LHCII chlorophyll protein complex, *FEBS Lett. 292*, 1−4.
4. Liu, Z. F., Yan, H. C., Wang, K. B., Kuang, T. Y., Zhang, J. P., Gui, L. L., An, X. M., and Chang, W. R. (2004) Crystal structure of spinach major light-harvesting complex at 2.72 Å resolution, *Nature 428*, 287−292.
5. Pascal, A. A., Liu, Z. F., Broess, K., van Oort, B., van Amerongen, H., Wang, C., Horton, P., Robert, B., Chang, W. R., and Ruban, A. (2005) Molecular basis of photoprotection and control of photosynthetic light-harvesting, *Nature 436*, 134−137.
6. Standfuss, R., van Scheltinga, A. C. T., Lamborghini, M., and Kuhlbrandt, W. (2005) Mechanisms of photoprotection and nonphotochemical quenching in pea light-harvesting complex at 2.5 Å resolution, *EMBO J. 24*, 919−928.
7. Jansson, S. (1994) The light-harvesting chlorophyll *a*/*b* binding proteins, *Biochim. Biophys. Acta 1184*, 1−19.
8. Caffarri, S., Croce, R., Cattivelli, L. and Bassi, R. (2004) A look within LHCII: differential analysis of the Lhcb 1-3 gene products composing the major antenna complex of higher plant photosynthesis, *Biochemistry 43*, 9467−9476.
9. Croce, R., Remelli, R., Varotto, C., Breton, J., and Bassi, R. (1999) The neoxanthin binding site of the major light harvesting complex (LHCII) from higher plants, *FEBS Lett. 456*, 1−6.
10. Remelli, R., Varotto, C., Sandona, D., Croce, R., and Bassi, R. (1999) Chlorophyll binding to monomeric light-harvesting complex−A mutation analysis of chromophore-binding residues, *J. Biol. Chem. 274*, 33510−33521.
11. Peterman, E. J. G., Gradinaru, C. C., Calkoen, F., Borst, J. C., van Grondelle, R., and van Amerongen, H. (1997) Xanthophylls in light-harvesting complex II of higher plants: Light harvesting and triplet quenching, *Biochemistry 36*, 12208−12215.
12. Novoderezhkin, V. I., Palacios, M. A., van Amerongen, H., and van Grondelle, R. (2005) Excitation dynamics in the LHCII complex of higher plants: Modeling based on the 2.72 angstrom crystal structure, *J. Phys. Chem. B 109*, 10493−10504.
13. Croce, R., Weiss, S., and Bassi, R. (1999) Carotenoid-binding sites of the major light-harvesting complex II of higher plants, *J. Biol. Chem. 274*, 29613−29623.
14. Nussberger, S., Dekker, J. P., Kuhlbrandt, W., van Bolhuis, B. M., van Grondelle, R., and van Amerongen, H. (1994) Spectroscopic characterization of 3 different monomeric forms of the main chlorophyll *a*/*b* binding-protein from chloroplast membranes, *Biochemistry 33*, 14775−14783.
15. Caffarri, S., Croce, R., Breton, J., and Bassi, R. (2001) The major antenna complex of photosystem II has a xanthophyll binding site not involved in light harvesting, *J. Biol. Chem. 276*, 35924−35933.
16. Ruban, A. V., Lee, P. J., Wentworth, M., Young, A. J., and Horton, P. (1999) Determination of the stoichiometry and strength of binding of xanthophylls to the photosystem II light harvesting complexes, *J. Biol. Chem. 274*, 10458−10465.
17. Hobe, S., Prytulla, S., Kühlbrandt, W., and Paulsen, H. (1994) Trimerization and crystallization of reconstituted light-harvesting chlorophyll *a*/*b* complex, *EMBO J. 13*, 3423−3429.
18. Ruban, A. V., Calkoen, F., Kwa, S. L. S., van Grondelle, R., Horton, P., and Dekker, J. P. (1997) Characterisation of LHC II in the aggregated state by linear and circular dichroism spectroscopy, *Biochim. Biophys. Acta 1321*, 61−70.
19. Renger, T., and May, V. (2000) Simulations of frequency-domain spectra: Structure-function relationships in photosynthetic pigment-protein complexes, *Phys. Rev. Lett. 84*, 5228.

20. Georgakopoulou, S., van der Zwan, G., Olsen, J. D., Hunter, C. N., Niederman, R. A., and van Grondelle, R. (2006) Investigation of the effects of different carotenoids on the absorption and CD signals of light harvesting 1 complexes, *J. Phys. Chem. B 110*, 3354−3361.
21. Georgakopoulou, S., van Grondelle, R., and van der Zwan, G. (2006) Explaining the visible and near-infrared circular dichroism spectra of light-harvesting 1 complexes from purple bacteria: A modeling study, *J. Phys. Chem. B 110*, 3344−3353.
22. Georgakopoulou, S., Frese, R. N., Johnson, E., Koolhaas, C., Cogdell, R. J., van Grondelle, R., and van der Zwan, G. (2002) Absorption and CD spectroscopy and modeling of various LH2 complexes from purple bacteria, *Biophys. J. 82*, 2184−2197.
23. Georgakopoulou, S., van Grondelle, R., and van der Zwan, G. (2004) Circular dichroism of carotenoids in bacterial light-harvesting complexes: Experiments and modeling, *Biophys. J. 87*, 3010−3022.
24. Koolhaas, M. H. C., van der Zwan, G., and van Grondelle, R. (2000) Local and nonlocal contributions to the linear spectroscopy of light-harvesting antenna systems, *J. Phys. Chem. B 104*, 4489−4502.
25. Koolhaas, M. H. C., Frese, R. N., Fowler, G. J. S., Bibby, T. S., Georgakopoulou, S., van der Zwan, G., Hunter, C. N., and van Grondelle, R. (1998) Identification of the upper exciton component of the B850 bacteriochlorophylls of the LH2 antenna complex, using a B800-free mutant of *Rhodobacter sphaeroides*, *Biochemistry 37*, 4693−4698.
26. Koolhaas, M. H. C., van der Zwan, G., Frese, R. N., and van Grondelle, R. (1997) Red shift of the zero crossing in the CD spectra of the LH2 antenna complex of *Rhodopseudomonas acidophila*: A structure-based study, *J. Phys. Chem. B 101*, 7262−7270.
27. van Amerongen, H., Kwa, S. L. S., van Bolhuis, B. M., and van Grondelle, R. (1994) Polarized fluorescence and absorption of macroscopically aligned light-harvesting complex-II, *Biophys. J. 67*, 837−847.
28. Georgakopoulou, S., Cogdell, R. J., van Grondelle, R., and van Amerongen, H. (2003) Linear-dichroism measurements on the LH2 antenna complex of *Rhodopseudomonas acidophila* strain 10050 show that the transition dipole moment of the carotenoid rhodopin glucoside is not collinear with the long molecular axis, *J. Phys. Chem. B 107*, 655−658.
29. Mukamel, S. (1995) *Principles of Nonlinear Optical Spectroscopy*, Oxford University Press, New York.
30. Porra, R. J. (1991) Recent advances and re-assessments in chlorophyll extraction and assay procedures for terrestrial, aquatic and marine organisms, including recalcitrant algae, in *Chlorophylls* (Scheer, H., Ed.) p 31, CRC press, Boca Raton, FL.
31. Palacios, M. A., de Weerd, F. L., Ihalainen, J. A., van Grondelle, R., and van Amerongen, H. (2002) Superradiance and exciton (de)-localization in light-harvesting complex II from green plants?, *J. Phys. Chem. B 106*, 5782−5787.
32. van Amerongen, H., and van Grondelle, R. (2001) Understanding the energy transfer function of LHCII, the major light-harvesting complex of green plants, *J. Phys. Chem. B 105*, 604−617.
33. Knox, R. S. (2003) Dipole and oscillator strengths of chromophores in solution, *Photochem. Photobiol. 77*, 492−496.
34. Norden, B., Fragata, M., and Kurucsev, T. (1992) X-polarized and Y-polarized spectra of chlorophyll-*a* and pheophytin-*a* in the red region−Resolution enhancement and gaussian deconvolution, *Aust. J. Chem. 45*, 1559−1570.
35. Fragata, M., Norden, B., and Kurucsev, T. (1988) Linear dichroism (250−700 nm) of chlorophyll-*a* and pheophytin-*a* oriented in a lamellar phase of glycerylmonooctanoate H_2O−Characterization of electronic-transitions, *Photochem. Photobiol. 47*, 133−143.
36. Simonetto, R., Crimi, M., Sandona, D., Croce, R., Cinque, G., Breton, J., and Bassi, R. (1999) Orientation of chlorophyll transition moments in the higher-plant light-harvesting complex CP29, *Biochemistry 38*, 12974−12983.
37. Vaitekonis, S., and Trinkunas, G. (2001) The orientation of the Qy transition dipole moment of chlorophyll *a* molecule in protein, *Lith. J. Phys. 41*, 169−173.
38. van Gurp, M., van der Heide, U., Verhagen, J., Piters, T., van Ginkel, G., and Levine, Y. K. (1989) Spectroscopic and orientational properties of chlorophyll-*a* and chlorophyll-*b* in lipid-membranes, *Photochem. Photobiol. 49*, 663−672.
39. van Zandvoort, M. A. M. J., Wrobel, D., Lettinga, P., van Ginkel, G., and Levine, Y. K. (1995) The orientation of the transition dipole-moments of chlorophyll-*a* and pheophytin *a* in their molecular frame, *Photochem. Photobiol. 62*, 299−308.
40. Kleima, F. J., Hofmann, E., Gobets, B., van Stokkum, I. H. M., van Grondelle, R., Diederichs, K., and van Amerongen, H. (2000) Forster excitation energy transfer in peridinin-chlorophyll-*a*-protein, *Biophys. J. 78*, 344−353.
41. Somsen, O. J. G., van Grondelle, R., and van Amerongen, H. (1996) Spectral broadening of interacting pigments: Polarized absorption by photosynthetic proteins, *Biophys. J. 71*, 1934.
42. van Amerongen, H., Valkunas, L., and van Grondelle, R. (2000) Mixing with higher excited states, in *Photosynthetic Excitons*, p 119, World Scientific, Singapore.
43. Schenkl, S., van Mourik, F., van der Zwan, G., Haacke, S., and Chergui, M. (2005) Probing the ultrafast charge translocation of photoexcited retinal in bacteriorhodopsin, *Science 309*, 917−920.
44. Gasymov, O. K., Abduragimov, A. R., Yusifov, T. N., and Glasgow, B. J. (2003) Resolving near-ultraviolet circular dichroism spectra of single trp mutants in tear lipocalin, *Anal. Biochem. 318*, 300−308.
45. Croce, R., Breton, J., and Bassi, R. (1996) Conformational changes induced by phosphorylation in the CP29 subunit of photosystem II, *Biochemistry 35*, 11142.
46. Mozzo, M., Morosinotto, T., Bassi, R., and Croce, R. (2006) Probing the structure of Lhca3 by mutation analysis, *Biochim. Biophys. Acta 1757*, 1607−1613.
47. Jackowski, G., and Pielucha, K. (2001) Heterogeneity of the main light-harvesting chlorophyll *a*/*b*-protein complex of photosystem II (LHCII) at the level of trimeric subunits, *J. Photochem. Photobiol., B 64*, 45−54.
48. Garab, G., Cseh, Z., Kovacs, L., Rajagopal, S., Varkonyi, Z., Wentworth, M., Mustardy, L., Der, A., Ruban, A. V., Papp, E., Holzenburg, A., and Horton, P. (2002) Light-induced trimer to monomer transition in the main light-harvesting antenna complex of plants: Thermo-optic mechanism, *Biochemistry 41*, 15121−15129.
49. Ide, J. P., Klug, D. R., Kühlbrandt, W., Giorgi, L. B., and Porter, G. (1987) The state of detergent solubilized light-harvesting chlorophyll-*a*/*b* protein complex as monitored by picosecond time-resolved fluorescence and circular-dichroism, *Biochim. Biophys. Acta 893*, 349−364.
50. Bassi, R., Silvestri, M., Dainese, P., Moya, I., and Giacometti, G. M. (1991) Effects of a nonionic detergent on the spectral properties and aggregation state of the light-harvesting chlorophyll-*a*/*b* protein complex (LHCII), *J. Photochem. Photobiol., B 9*, 335−354.
51. Barzda, V., Gulbinas, V., Kananavicius, R., Cervinskas, V., van Amerongen, H., van Grondelle, R., and Valkunas, L. (2001) Singlet-singlet annihilation kinetics in aggregates and trimers of LHCII, *Biophys. J. 80*, 2409−2421.

BI062031Y